Journal of Applied Polymer Science

Design of a Probe Based on Poly(glycidyl methacrylate-*co*-vinylferrocene)-Coated Pt Electrode for Electrochemical Detection of PTEN Gene in PCR Amplified Samples from Prostate Tissues

Salih Zeki Bas,[1] Esra Maltas,[1] Busra Sennik,[2,3] Faruk Yilmaz,[3] Hasibe Cingilli Vural[4]

[1]Department of Chemistry, Selcuk University, 42075, Selcuklu, Konya, Turkey
[2]Department of Chemistry, Istanbul Medeniyet University, 34720, Kadikoy, Istanbul, Turkey
[3]Department of Chemistry, Gebze Institute of Technology, 41400, Gebze, Kocaeli, Turkey
[4]Department of Biology, Selcuk University, 42075, Selcuklu, Konya, Turkey
Correspondence to: S. Z. Bas (E-mail: salihzekibas@gmail.com)

ABSTRACT: In this study, a new probe based on immobilization of amino linked oligonucleotide (NH_2-linked DNA) on poly(glycidyl methacrylate-*co*-vinylferrocene)-coated Pt electrode was fabricated for the electrochemical detection of PTEN gene from human prostate tissues. The experimental parameters such as DNA immobilization time, DNA concentration, and target concentration were optimized. The selectivity of the NH_2-linked DNA probe was assessed with mismatch (MM) and noncomplementary (NC) sequences. The applicability of the NH_2-linked DNA probe to the PCR amplified samples correspond to PTEN gene from prostate tissues was evaluated. The immobilization of DNA on the copolymer was confirmed by FTIR, AFM, CV and DPV analysis. The PCR products were also identified by using agarose gel electrophoresis. The prepared probe indicated a linear range (10–100 μg mL^{-1}) with a detection limit (4.7 μg mL^{-1}) and a good selectivity of the NH_2-linked DNA probe toward target DNA sequence. © 2014 Wiley Periodicals, Inc. J. Appl. Polym. Sci. **2014**, *131*, 40638.

KEYWORDS: biomaterials; nucleic acids; sensors and actuators

Received 13 December 2013; accepted 26 February 2014
DOI: 10.1002/app.40638

INTRODUCTION

PTEN, a unique tumor suppressor gene, (also known as MMAC1 or TEP1) has recently been isolated from chromosome 10q23.3.[1] This gene inactivates many different types of cancers including glioma, melanoma, and carcinoma of the endometrium, kidney, prostate, breast, and lung.[2] The activity of PTEN is related to its ability to dephosphorylate phosphoproteins or phospholipids and negatively regulate the activity of the phosphatidylinositol 3-kinase pathway. Loss of PTEN activity as a tumor suppressor gene increases the cell proliferation and the tumor angiogenesis, thus, decreases apoptosis.[3] There are some reports on PTEN gene mutation and protein expression in many tumor types such as lung, breast cancer and prostate cancer.[4–6] One of the cancer types, prostate cancer is classified as the most commonly diagnosed cancer among the men. The current prognostic tools such as preoperative prostate specific antigen (PSA) levels and histological Gleason grading of biopsy specimens are not available to determine risk stratify of individual patients with prostate cancer at early stages of the disease.[7] The prostate cancer model by PTEN has been described for diagnosis in the initiation of prostate cancer with prostatic intraepithelial neoplasia (PIN), followed by progression to invasive adenocarcinoma, and subsequent metastasis.[8–10] Identification of specific DNA sequence related to any disease will enable the development of new methods. The detection of specific DNA squence is a basis to the diagnosis and the treatment of various diseases as well as many applications in genetics, pathology, criminology, pharmacogenetics, and food safety.[11,12] In molecular diagnostic researches based on the analysis of DNA sequence, a variety of the detection methods such as fluorescent,[13] electrophoresis,[14] electrochemiluminecence,[15,16] quartz crystal microbalance,[17] electrochemical impedance spectroscopy,[18–21] voltammetry[21–25] have been developed. Compared with the other methods, the electrochemical detection of DNA provides an advantage due to high sensitivity, low cost, rapid, portability, and compatibility with micro-fabrication technology.[26] The effective features of the electrochemical methods allows widely for improving a great variety of DNA biosensors. In the literature, some techniques for the electrochemical detection of the DNA hybridization have been reported. The hybridization can be detected directly,[27] by using a redox indicator,[28,29] intercalator,[30,31] enzyme,[32] nanoparticle,[33] or supporting material.[34,35]

In this study, to identify PTEN gene in prostate tissue, we developed a selective DNA biosensor for the detection of PTEN

Table I. Composition Data for Copolymerization of GMA with VFc

Copolymer	Monomer feed ratio	M_n (GPC)[a]	M_w/M_n	VFc in copolymer (mol %)[b]
P(GMA_{92}-*co*-VFc_8)	75/25	42,000	3.7	8
P(GMA_{87}-*co*-VFc_{13})	50/50	11,000	2.8	13
P(GMA_{85}-*co*-VFc_{15})	25/75	3,000	1.7	15

Temperature: 65°C, bulk, polymerization time: 24 h.
[a] Polystyrene standards were used to determine M_n and M_w/M_n of the copolymer.
[b] Mole fraction of VFc in the copolymer was determined by UV-Vis spectrophotometer using different concentrations of ferrocene solutions in THF as the standard solutions.

gene using poly(glycidyl methacrylate-*co*-vinylferrocene) having pendant epoxy and ferrocene groups. Previously, this copolymer was employed as a polymeric mediator for the construction of biosensor based on tyrosinase,[36] glucose oxidase,[37] galactose oxidase,[38] horseradish perosidase[39] enzymes. The DNA detection was carried out monitoring the change in the oxidation signal of the modified copolymer before and after the hybridization without using any redox indicator. The effect of DNA immobilization time, target concentration and DNA concentration on the current response of the biosensing system were examined by using CV and DPV techniques. In addition, the proposed probe was applied to the electrochemical analysis of PTEN gene in PCR samples obtained from prostate tissues.

EXPERIMENTAL

Reagents

Glycidyl methacrylate (GMA, 97%) and vinylferrocene(VFc, 97%) were purchased from Sigma (St. Louis, MO). GMA was purified by distillation under reduced pressure. α,′-azobisisobutyronitrile (AIBN, 98%) (Sigma, St. Louis, MO) was purified by recrystallization from methanol. Dichloromethane (99%) was obtained from Merck (Darmstadt, Germany). The 20-mer oligonucleotide (ODN) was purchased from Metabion International AG (Germany). The following base sequences were designed from PTEN gene sequence in human (Accession number: AF143313).

Amino linked probe: 5′-NH_2-TACGGTAAGCCAAAAAATGA

Target: 5′TCATTTTTTGGCTTACCGTA

Mismatch (MM): 5′TCATTTTTTGGCTTACAGTA

Noncomplementary (NC): 5′GAAAAGAAAGCTTTCCCCACTA

Calf thymus DNA(CT-DNA) was used for the preparation of the probe in the optimization studies. CT-DNA was purchased from Sigma (St. Louis, MO). CT-DNA stock solution (1 mg mL^{-1}) was prepared with ultrapure water and kept frozen (−20°C). The diluted solutions of CT-DNA and ODN were prepared by using phosphate buffer solution (PBS) (0.01*M*, pH 7). All other chemicals were of analytical grade and ultrapure water (Millipore Milli-Q Plus water purification system) was used for preparing all of the solutions.

Apparatus and Instrumentations

All electrochemical measurements were performed with a CHI-660C electrochemical workstation (CH Instruments Co., USA). A conventional three electrode system was used with platinum electrode (area: 0.0314 cm^2) as working electrode, a platinum wire as auxiliary electrode and an Ag/AgCl (3*M* KCl) electrode as reference electrode. Prior to each experiment, Pt electrode was polished with 0.05 μm alumina powder, and then ultrasonicated in deionized water. IR spectra were recorded on a Perkin-Elmer spectrum 100 FTIR spectrometer (ATR)(Perkin-Elmer Inc., USA). Atomic force microscopy (AFM) images were obtained by using Veeco diCaliber AFM(Veeco Inc., CA). The average molecular weights and the molecular weight distributions of the copolymer was determined on an Agilent 1100 GPC Instrument (Agilent Tech., USA) consisting of a pump, a refractive index detector and two Waters Styragel columns and using THF as eluent at a flow rate of 0.5 mL min^{-1} at 23°C. ^{1}HNMR spectra was recorded in $CDCl_3$ solution on a Varian UNITY INOVA 500 MHz spectrometer. UV–vis was recorded using 1-cm path length cuvettes on Shimadzu 2001UV.

Synthesis of P(GMA-co-VFc)

P(GMA-*co*-VFc) was prepared by conventional free-radical copolymerization GMA and VFc monomers initiated by α,α′-azobisisobutyronitrile (AIBN) as reported previously.[36] GMA (1.40 g, 9 mmol), VFc (0.690 g, 3 mmol), and AIBN (10 mg, 0.5% of total weight of monomers) were put in a Pyrex tube. The reaction mixture was degassed by gently purging with oxygen-free argon for 10 min. After the tube was tightly sealed, it was immersed into an oil bath previously thermostated to 65°C and stirred 24 h. After the completion of the reaction, the copolymer was precipitated from methanol and was filtered. The product was dried under reduced pressure until a constant weight. The copolymerization conditions and the composition data of P(GMA-*co*-VFc) prepared in this study were given in Table I.

DNA Immobilization and Hybridization

The copolymer film was prepared by the drop-coating method on the surface of Pt electrode with 5 μL of 1 mg mL^{-1} P(GMA-*co*-VFc) solution in dichloromethane and dried in air at room temperature. The copolymer-coated Pt electrode(P(GMA-*co*-VFc)/Pt) was immersed in 0.01*M* PBS (pH 7) for 1 h, and then kept in 200 μg mL^{-1} NH_2-linked DNA solution for the DNA immobilization for 6 h at 4°C. Finally, NH_2-linked DNA probe was washed lightly with 0.01*M* PBS for 10 s to remove the unbound DNA prior to use. The preparation of NH_2-linked DNA probe was schematically shown in Scheme 1. After the immobilization of NH_2-linked DNA on P(GMA-*co*-VFc)/Pt electrode, the hybridization with target was performed by immersing the probe into 100 μg mL^{-1} target solution for

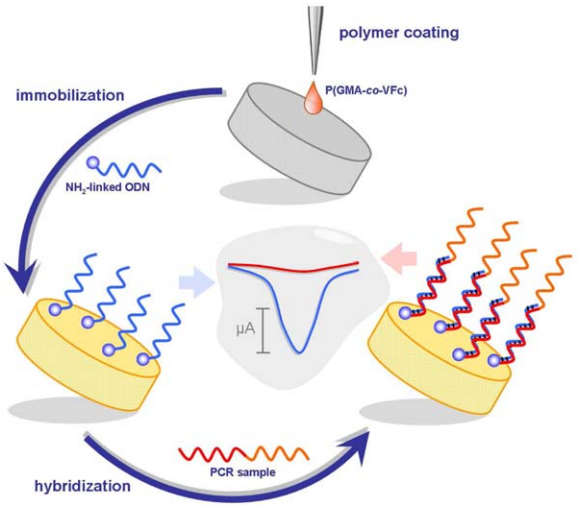

Scheme 1. Schematic illustration of fabrication of NH_2-linked DNA probe. [Color figure can be viewed in the online issue, which is available at wileyonlinelibrary.com.]

30 min. The hybridization with MM (100 μg mL^{-1}) and NC (100 μg mL^{-1}) was carried out using the same procedure as described above. In the hybridization studies with PCR samples amplified DNA from human prostate tissues, the denaturation of PCR products was occurred at 95°C for 8 min and 0°C for 5 min.[40] In the optimization studies, the immobilization of CT-DNA(Calf thymus DNA) on P(GMA-*co*-VFc)/Pt was carried out using the same procedure above.

Electrochemical Measurements

The oxidation signal of the copolymer before and after the hybridization was measured in 0.1*M* PBS containing 0.1*M* $NaClO_4$ by cyclic voltammetry(CV) between −0.1−1.0 V at a scan rate of 50 mV s^{-1}. Also, the electrochemical behavior of NH_2-linked DNA probe in the presence and the absence of target was investigated by using differential pulse voltammetry (DPV) between −0.1−1.0 V with amplitude of 50 mV. Similarly, CV and DPV techniques were used for the electrochemical behavior of CT-DNA immobilized P(GMA-*co*-VFc)/Pt electrode.

DNA Extraction from Prostate Tissue

Paraffin-embedded prostate tissue specimens were derived from the Faculty of Medicine at Necmettin Erbakan University, Turkey. DNA extracted from the paraffin blocks was carried out according to the procedure described by Vural et al.[41]

PCR Amplification of PTEN Gene

PCR(polymerase chain reaction) was performed using 100 ng of genomic DNA extracted from prostate tissue and specific primer according to the procedure described by Vural et al.[41] 5′TGACCACCTTTTATTACTCCA-3' (forward) and 5′TACGGTAAGCCAAAAAATGA-3' (reverse) were used as primers (1 m*M* each) in a 25 μL PCR mix containing 5 μL 10XPCR, Taq buffer (pH 8.8), 2 mmol L^{-1} $MgCl_2$, and 10 mmol L^{-1} of each dNTP (dGTP, dATP, dTTP, dCTP), 0.5 mmol L^{-1} of each primer, and 0.3 U DreamTaq polymerase (Advanced Biotechnologies, Fermantase Life Science). Amplifications were performed using an automatic thermocycler (Biorad company, Germany) as follows: initial denaturation at 94°C for 4 min, denaturation at 94°C for 15 s, annealing at 60°C for 30 s, extension at 72°C for 15 s followed by 10 cycles and denaturation at 94°C for 15 s, annealing at 58°C for 20 s, extension at 72°C for 15 followed by 20 cycles, end step at 72°C for 3 min final extension. The PCR products were separated by gel electrophoresis system (Biorad Company, Germany) in a 2% agarose solution containing ethidium bromide and were imaged on Quantum ST4 UV transsimilator(Vilber Lourmat, France).

RESULTS AND DISCUSSION

The detection of DNA based on the electrochemical behavior of the supporting material arising from redox couple has been successfully applied to the process of the immobilized electrodes.[35,42,43] Additionally, another method used for the DNA detection is based on monitoring the change in the current response of the electroactive materials such as $Co(bpy)_3^{3+}$[44] and $Fe(CN)_6^{3-/4-}$[45,46] with the hybridization of the target DNA squence to the DNA probe. For this reason, we used a redox copolymer (poly(glycidyl methacrylate-*co*-vinylferrocene)(P(GMA-*co*-VFc)) containing pendant epoxy and ferrocene moieties as a supporting material for DNA detection. The epoxy and ferrocene moieties of P(GMA-*co*-VFc) were employed for direct immobilization of DNA and electron transfer mediator in the fabrication of DNA biosensor, respectively. Thus, the electrochemical detection was carried out by measuring the oxidation signals of VFc unit in the structure of the copolymer without the need to any electroactive material.

FTIR, ^{1}HNMR, and UV Analysis

The immobilization of DNA on the copolymer was confirmed by FTIR spectroscopy comparing the spectra of structures before and after the immobilization process [Figure 1(I)] The strong sharp peak at 1724 cm^{-1} comes from vibrations of carbonyl bonds of the copolymer.[36] Ferrocene ring absorptions at 998 and 1106 cm^{-1} indicate that the unsubstituted ferrocene ring is unaffected by the copolymerization reactions.[36] The symmetric ring stretching frequency of the epoxy ring in the copolymer structure occurs around 906 cm^{-1}.[36] After the immobilization of CT-DNA on the copolymer, a new peak in the spectrum of DNA immobilized on the copolymer appears at 1037 cm^{-1} which is attributable to phosphate backbone of the oligonucleotide. It is also observed that there are new small peaks at 1629, 1586 in the spectrum of DNA immobilized on the copolymer which are assigned to C═N stretching vibrations of DNA bases.[34,47] The peak at 1552 cm^{-1} is related to the C—N and C—C stretching vibration modes of the purine ring.[48]

The composition analysis was performed at 440 nm (attributed to the ferrocenyl moiety). UV-Vis spectrum of the copolymer is shown in Figure 1(II). The copolymer shows two characteristic absorption peaks at 335 nm and 440 nm resulting from the ring MO-MO* transition and the d-d* transitions, respectively.

The chemical structure of the copolymer was also characterized by ^{1}HNMR spectroscopic method. The ^{1}HNMR spectrum of poly(GMA_{92}-*co*-VFc_8) obtained from a comonomer mixture with a feed ratio of [GMA]/[VFc] = 1.15 is shown in Figure 1(III).

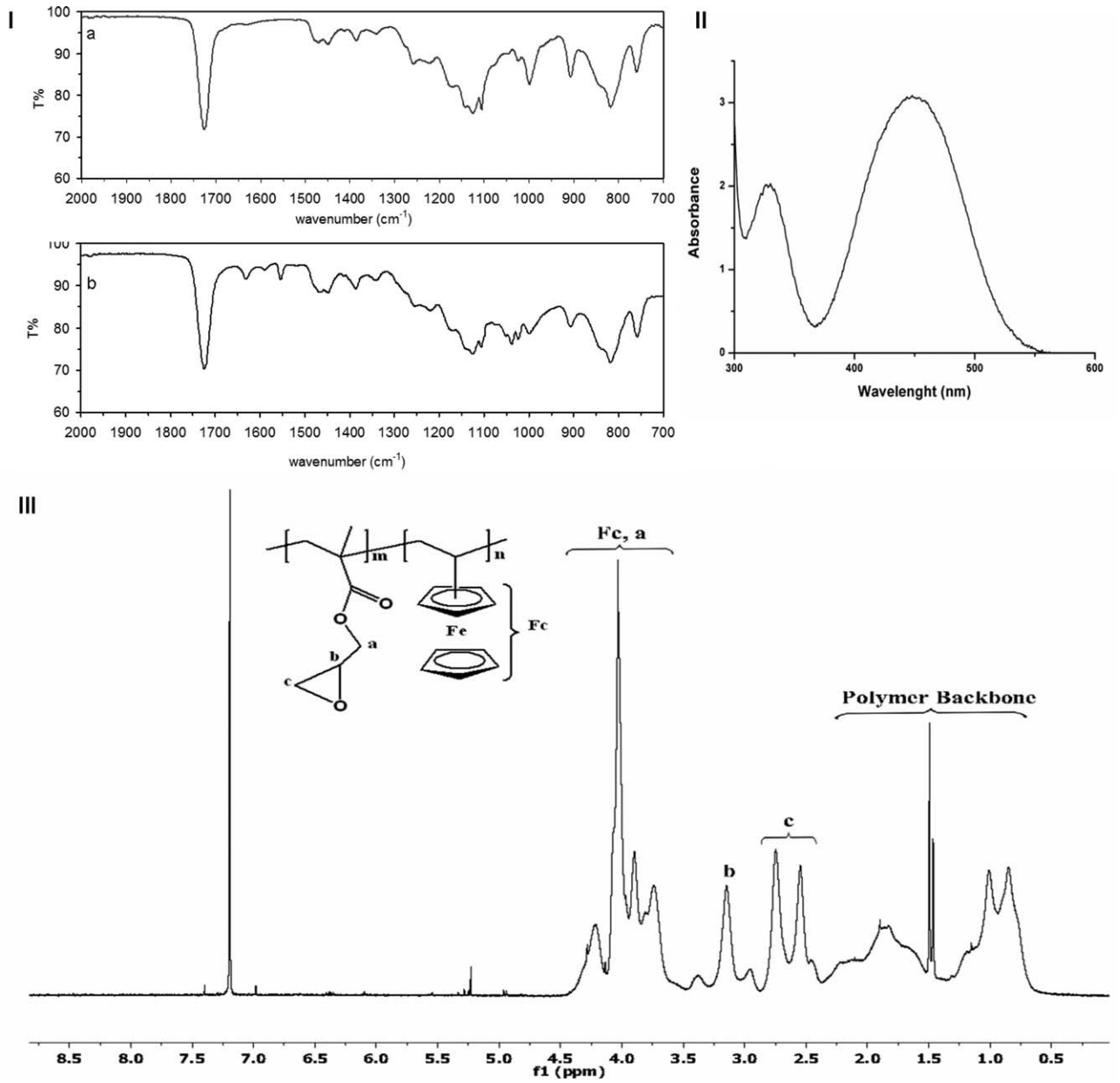

Figure 1. (I) FTIR spectra of P(GMA-*co*-VFc)(a) and CT-DNA immobilized P(GMA-*co*-VFc)(b), (II) UV-vis spectrum and (III) ^{1}H-NMR spectrum of P(GMA-*co*-VFc).

The chemical shift assignments of the copolymers were based on those obtained for GMA and VFc monomers.

AFM Analysis

Atomic force microscopy(AFM) imaging technique is used to image DNA, which plays an important role in molecular biology, with high accuracy.[49,50] Thus, after the immobilization of DNA, we was examined the topographical analysis of CT-DNA immobilized on P(GMA-*co*-VFc) using AFM. The images were shown two- and three-dimensionally in Figure 2. In analyzing the results of AFM, the immobilization of DNA on the copolymer can be seen clearly in Figure 2(c) (including image with a scan area of 5 × 5 μm^2). The DNA width of AFM images in Figure 2(a,b) (3D and 2D images with a scan area of 1 × 1 μm^2) is about 10 nm, which is larger than the known molecular width of DNA due to the size of the probe tip used.[51] The results obtained from the AFM images show that it is possible to immobilize DNA molecules on the copolymer-coated Pt electrode.

Optimization Studies

Figure 3 shows CVs of P(GMA-*co*-VFc)/Pt and CT-DNA immobilized P(GMA-*co*-VFc)/Pt electrode at potential range of −0.1−1.0 V at scan rate of 50 mV s^{-1} in 0.1*M* PBS containing 0.1*M* $NaClO_4$. The oxidation of VFc unit was recorded at +0.37 V, corresponding to the reversible one electron

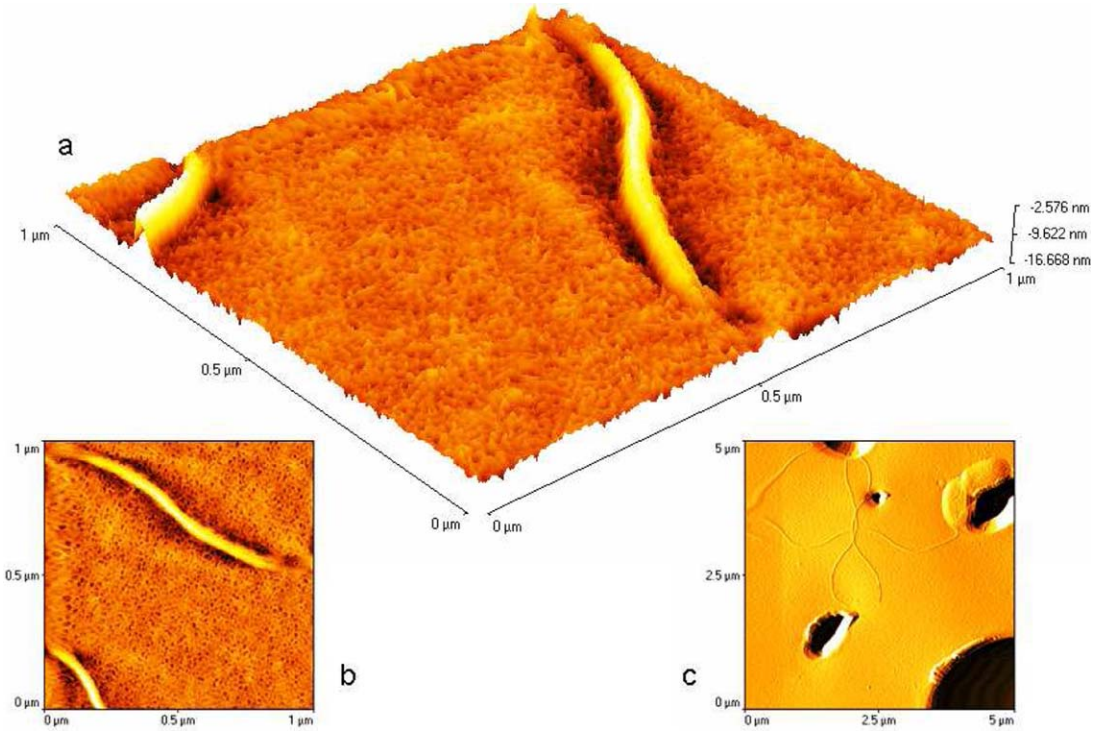

Figure 2. AFM images of CT-DNA immobilized on P(GMA-*co*-VFc). (a and b) three- and two-dimensional view with a scan area of 1 × 1 μm^2, (c) two-dimensional view with a scan area of 5 × 5 μm^2. [Color figure can be viewed in the online issue, which is available at wileyonlinelibrary.com.]

reduction of VFc^+ with a peak potential of +0.14 V, which was assigned to the ferrocenium/ferrocene (Fc^+/Fc) couple [Figure 3(I)]. The oxidation and the reduction peak currents of CT-DNA immobilized P(GMA-*co*-VFc)/Pt electrode decreased as compared with that of P(GMA-*co*-VFc)/Pt electrode [Figure 3(II)]. This result may be attributed to blocking of the electroactive sites of VFc^+ by CT-DNA during the immobilization of CT-DNA on P(GMA-*co*-VFc)/Pt electrode. The electrochemical behavior of P(GMA-*co*-VFc)/Pt and CT-DNA immobilized P(GMA-*co*-VFc)/Pt electrodes was also investigated by using DPV between −0.1−1.0 V with amplitude of 50 mV in 0.1 M PBS containing 0.1*M* $NaClO_4$ (inset of Figure 3). The oxidation peak of P(GMA-*co*-VFc)/Pt was observed at +0.32 V. The oxidation peak current of the CT-DNA immobilized P(GMA-*co*-VFc)/Pt electrode decreased after the immobilization of CT-DNA on P(GMA-*co*-VFc)/Pt electrode. The results were similar to the results obtained from the CV of the immobilized electrode.

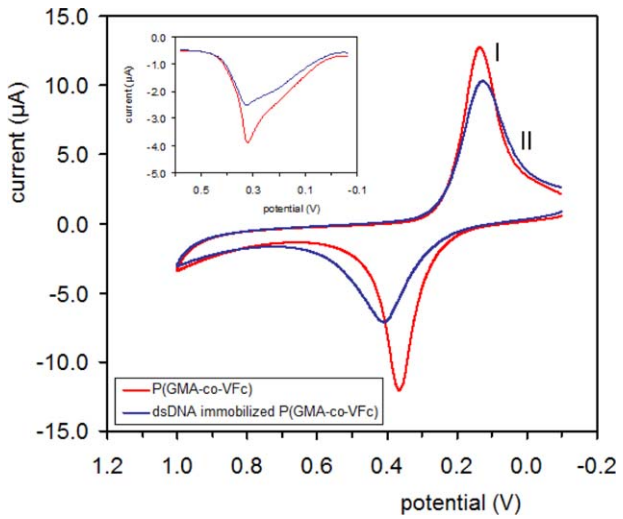

Figure 3. CVs of P(GMA-*co*-VFc)/Pt(I) and CT-DNA immobilized P(GMA-*co*-VFc)/Pt(II) in 0.1*M* PBS containing 0.1*M* $NaClO_4$ at scan rate of 50 mV s^{-1}. Inset: DPVs of P(GMA-*co*-VFc)/Pt(I) and CT-DNA immobilized P(GMA-*co*-VFc)/Pt(II) in 0.1*M* PBS containing 0.1*M* $NaClO_4$ at amplitude of 50 mV. CT-DNA concentration: 700 $\mu g\ mL^{-1}$, immobilization time: 5 h. [Color figure can be viewed in the online issue, which is available at wileyonlinelibrary.com.]

The effect of the percentage of VFc on the current response of the probe was examined. For this, the copolymers of VFc with GMA at different monomer ratios were synthesized by conventional free radical polymerization method. The copolymerization conditions and the composition data of the copolymers were given in Table I. Then, CT-DNA immobilized electrode was prepared using the copolymers with different percent VFc (8, 13, and 15%). For the DNA immobilization step, P(GMA-*co*-VFc)/Pt electrodes were immersed in 200 $\mu g\ mL^{-1}$ CT-DNA solution for 6 h at 4°C. According to the result of CV experiments, the decrease in the current response of the CT-DNA immobilized P(GMA-*co*-VFc)/Pt electrodes were found to be 6.9% for P(GMA_{92}-*co*-VFc_8), 15.1% for P(GMA_{87}-*co*-VFc_{13}), and 16.2% for P(GMA_{85}-*co*-VFc_{15}) when the response of the copolymer-coated electrode was taken as 100%. This result revealed that the peak current of the CT-DNA immobilized

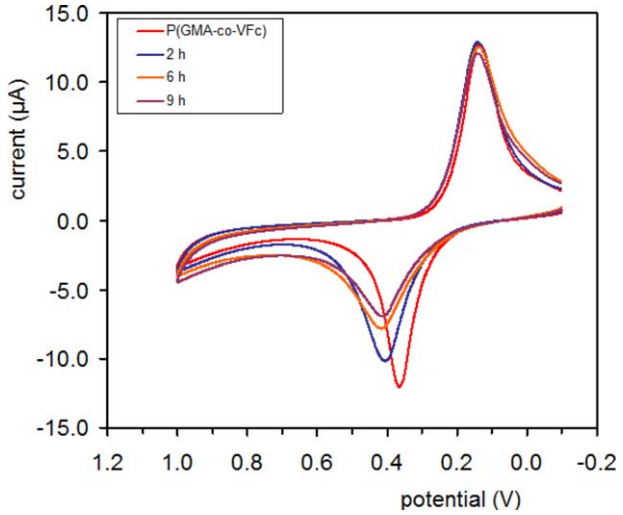

Figure 4. CVs of P(GMA-*co*-VFc)/Pt and CT-DNA immobilized P(GMA-*co*-VFc)/Pt prepared at the immobilization time of 2, 6, and 9 h. Scan rate: 50 mV s^{-1}. CT-DNA concentration: 500 μg mL^{-1}. [Color figure can be viewed in the online issue, which is available at wileyonlinelibrary.com.]

P(GMA-*co*-VFc)/Pt electrode decreased with the increase of percentage of VFc in the structure of the copolymer due to the increase of the amount of immobilized CT-DNA.

The amount of CT-DNA on the copolymer surface depends on the immobilization time of DNA and the concentration of the DNA solution used during immobilization process.[22,34,47,52] The effect of immobilization time on the peak current of the modified electrode was also tested at different immobilization time of 2–9 h. The CV peaks of this study are shown in Figure 4. With increasing immobilization time, the peak current of the CT-DNA immobilized P(GMA-*co*-VFc)/Pt electrode decreased slowly due to the increase in the amount of CT-DNA loading on the polymer-modified electrode.

To investigate the effect of the DNA concentration on the response of biosensor, the CT-DNA immobilized P(GMA-*co*-VFc)/Pt electrode were prepared with the CT-DNA concentrations varying between 150 and 2200 μg mL^{-1}. Figure 5(a,b) present the CV and DPV results obtained for the CT-DNA immobilized P(GMA-*co*-VFc)/Pt electrodes prepared with the different concentrations of CT-DNA. Compared with P(GMA-*co*-VFc)/Pt electrode, the oxidation signals of the CT-DNA immobilized P(GMA-*co*-VFc)/Pt gradually decreased, which is extremely important for a sensor application. It indicates that the binding amount of CT-DNA on P(GMA-*co*-VFc)/Pt electrode increased with increasing of the CT-DNA concentration. Inset of Figure 5(b) shows the change in the oxidation signals of the CT-DNA immobilized P(GMA-*co*-VFc)/Pt electrode as a function of CT-DNA concentration used for immobilization. The oxidation peak current of CT-DNA immobilized P(GMA-*co*-VFc)/Pt electrode showed a linear relationship in the CT-DNA concentration range of 150–1400 μg mL^{-1} ($R^2 = 0.9832$). When the concentration of CT-DNA was higher than 1400 μg mL^{-1}, the oxidation peak current did not change appreciably because of the saturation value of P(GMA-*co*-VFc) structure at this concentration value.[34]

Hybridization Studies

Amino linked 20-mer oligonucleotid was used as model DNA to investigate the applicability of the biosensor to the PCR samples. Amino linked oligonucleotid (NH_2-linked DNA) was immobilized on the copolymer film by immersing the modified Pt electrode in NH_2-linked DNA solution for 6 h at 4°C (defined as NH_2-linked DNA probe). First, the change in the oxidation peak current of the probe prepared with the different concentrations (25–800 μg mL^{-1}) of NH_2-linked DNA was examined. As shown in Figure 6, the DPV peak current of the NH_2-linked DNA probe was found to decrease with the concentration of NH_2-linked DNA and then, remained constant after a concentration of 600 μg mL^{-1}. The oxidation signal of the

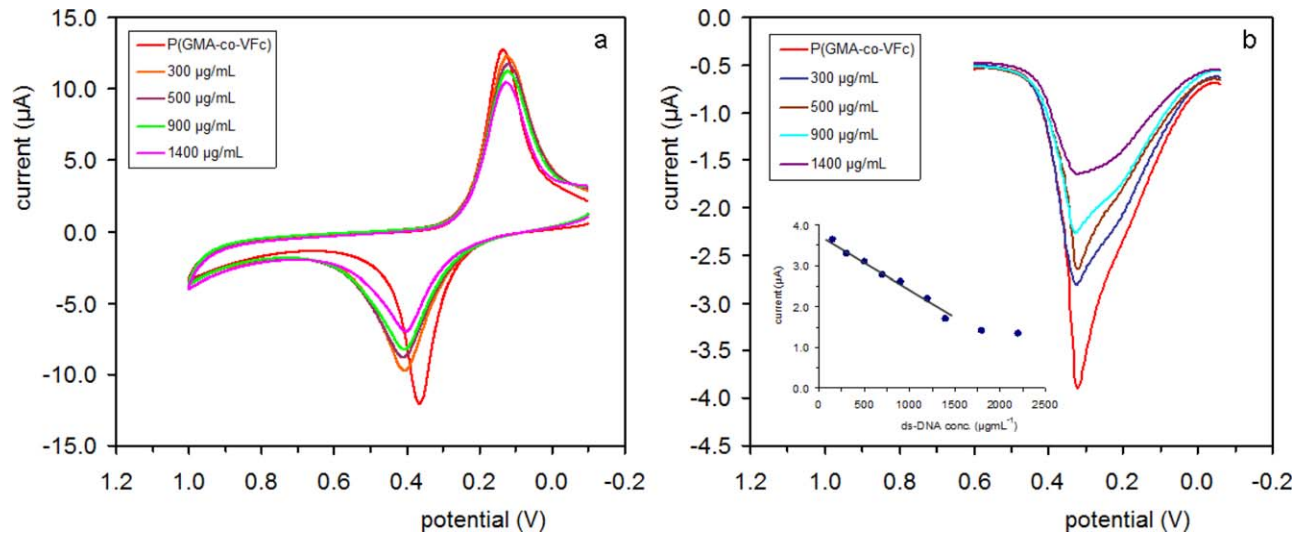

Figure 5. (a) CVs of P(GMA-*co*-VFc)/Pt and CT-DNA immobilized P(GMA-*co*-VFc)/Pt prepared with CT-DNA concentration of 300, 500, 900, and 1400 μg mL^{-1}. Scan rate: 50 mV s^{-1}. Immobilization time: 6 h. (b) DPVs of P(GMA-*co*-VFc)/Pt and CT-DNA immobilized P(GMA-*co*-VFc)/Pt prepared with CT-DNA concentration of 300, 500, 900, and 1400 μg mL^{-1}. Amplitude: 50 mV. Immobilization time: 6 h. Inset of b: The effect of different concentration of CT-DNA on the response of the biosensor. [Color figure can be viewed in the online issue, which is available at wileyonlinelibrary.com.]

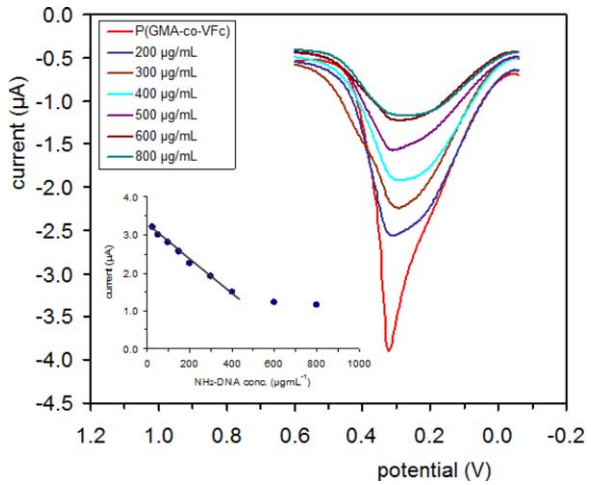

Figure 6. DPVs of P(GMA-*co*-VFc)/Pt and NH_2-linked DNA probe prepared with NH_2-linked DNA concentration of 200, 300, 400, 500, 600, and 800 μg mL^{-1}. Amplitude: 50 mV. Immobilization time: 6 h. Inset: The effect of different concentration of NH_2-linked DNA on the response of the biosensor. [Color figure can be viewed in the online issue, which is available at wileyonlinelibrary.com.]

NH_2-linked DNA probe was linear with the concentration of NH_2-linked DNA from 25 to 400 μg mL^{-1} with a correlation coefficient of 0.9923 (inset of Figure 6). The DPVs of the NH_2-linked DNA probe exhibit a decrease of peak current and an increase in the peak potential separation of the NH_2-linked DNA probe because the DNA molecules on the copolymer film provide a barrier for the electron transfer of the redox couple at the electrode.[53–55]

The recognition of the different DNA sequences such as noncomplementary (NC) and mismatch (MM) using the NH_2-linked DNA probe as well as the hybridization with the target sequence was examined by following the oxidation peak current of the modified electrode. The peak current decrease of about 1.30 μA (i.e., a current decrease of 54%) was observed after the hybridization of the NH_2-linked DNA probe with the target DNA sequence [Figure 7(a)]. To evaluate the selectivity of the biosensor, the control experiments for DNA hybridization were performed using a concentration of 100 μg mL^{-1} noncomplementary (NC) and 100 μg mL^{-1} mismatch (MM) DNA sequences [Figure 7(a,b)]. The concentration of target was 100 μg mL^{-1} for the studies related to NC and MM DNA sequences below. No or a negligible change in the peak current was observed on the NH_2-linked DNA probe, indicating that the NH_2-linked DNA probe was highly selective toward target DNA sequence. In the same time, this result confirmed that NC and MM DNA sequences could not hybridize with the NH_2-linked DNA probe. The analytical performance of the NH_2-linked DNA probe was further explored by using different concentrations (10–200 μg mL^{-1}) of the target sequence for the hybridization. As expected, the results for DPV experiments showed that the oxidation peak current of the NH_2-linked DNA probe decreased with increasing of the concentration of the target sequence as a result of the hybridization between the NH_2-linked DNA probe and its target sequence. Inset of Figure 7 shows the change in the oxidation currents of the probe as a function of the target concentration. The statistical analysis of the calibration curve of the NH_2-linked DNA probe gave the regression equation $y = -0.0171x + 2.8051$ with a correlation coefficient of 0.9817, where y is the current (μA) and x is the target concentration (μg mL^{-1}). The detection limit [at the signal-to-noise ratio of 3 ($S/N = 3$)] achieved with the NH_2-linked DNA probe was calculated to be 4.7 μg mL^{-1}. The relative standard deviation (RSD) was estimated 4.41% for three successive determinations of a 75 μg mL^{-1} target concentration, showing high regeneration and reproducibility of the developed DNA biosensor.

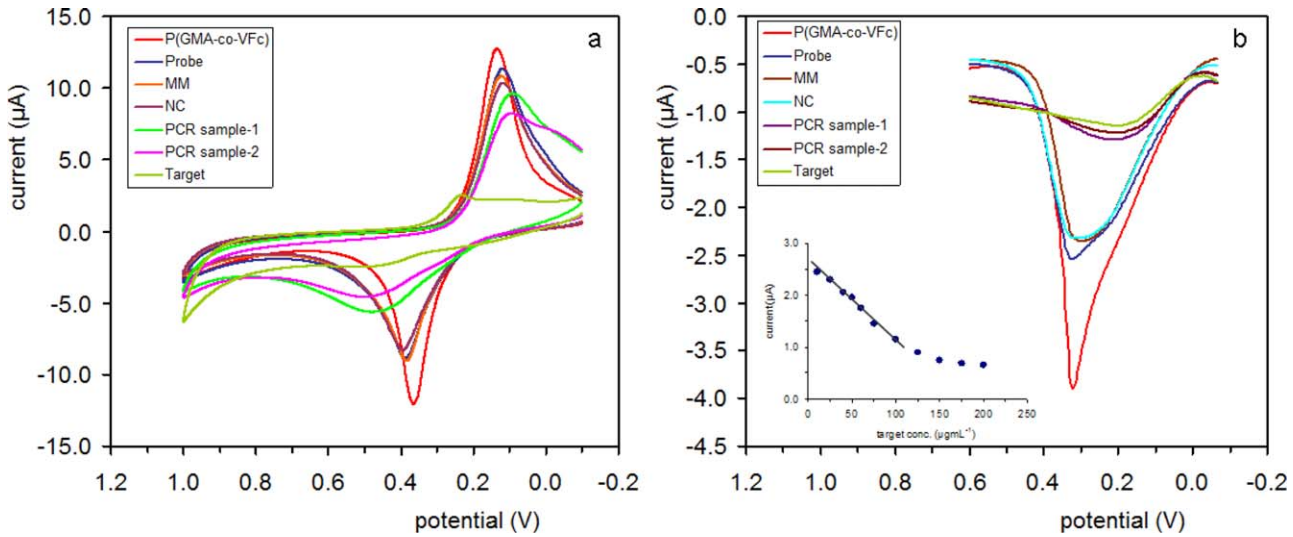

Figure 7. (a) CVs of P(GMA-*co*-VFc)/Pt and the hybridization between NH_2-linked DNA probe and target(100 μg mL^{-1}), MM(100 μg mL^{-1}), NC(100 μg mL^{-1}) and PCR-samples. Scan rate: 50 mV s^{-1}. Immobilization time: 6 h. Hybridization time: 30 min. (b) DPVs of P(GMA-*co*-VFc)/Pt and the hybridization between NH_2-linked DNA probe and target(100 μg mL^{-1}), MM(100 μg mL^{-1}), NC(100 μg mL^{-1}) and PCR-samples. Amplitude: 50 mV s^{-1}. Immobilization time: 6 h. Inset of b: The effect of different concentration of target on the response of the biosensor. [Color figure can be viewed in the online issue, which is available at wileyonlinelibrary.com.]

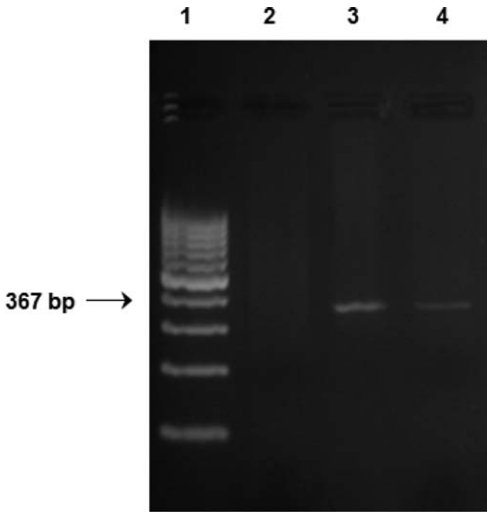

Figure 8. Agarose gel analysis of PCR samples. Lane 1: DNA marker, Lane 2: negative control, Lane 3: PCR sample-1, Lane 4: PCR sample-2.

To test the real applicability of our DNA biosensor, the hybridization between the NH_2-linked DNA probe and the target DNA sequences which are present in the PCR-amplified samples correspond to PTEN gene from human prostate tissues was determined by using the CV and DPV techniques in 0.1*M* PBS containing 0.1*M* $NaClO_4$. It was observed in Figure 7(a,b) that the oxidation peak currents of the NH_2-linked DNA probe hybridized with the PCR amplified samples decreased as compared with the NH_2-linked DNA probe. The decrease in the peak current reflects the extent of the hybridization formation at the probe. When the NH_2-linked DNA probe with the PCR amplified samples was hybridized, it was observed that the decrease in the peak current is 49% for PCR sample-1 and 52% for PCR sample-2 as compared with the NH_2-linked DNA probe. The concentrations of PTEN gene in the PCR samples were calculated to be 88.60 μg mL^{-1} for PCR sample-1 and 93.28 μg mL^{-1} for PCR sample-2 from the regression equation for the hybridization. In the detection of the PCR amplified samples, the results similar to that of target sequence were obtained, indicating that the method was also effective in determining long chain target DNA.[25] As a result, we can state clearly that the probe prepared using NH_2-linked oligonucleotide has a good selectivity toward both the target and the PCR-amplified samples obtained from prostate tissues.

The amplifications of DNA samples performed by PCR technique were also identified by using agarose gel electrophoresis. The electrophoresis method for the separation of PCR products was carried out in a 2% agarose gel in 1XTAE buffer (45 m*M* Tris, 1 m*M* EDTA, pH 8), stained with ethidium bromide. In the agarose gel analysis, as shown in Figure 8, PCR products from human prostate tissues which were used to be real samples to detect PTEN gene were amplified as 367 bp.

CONCLUSIONS

In conclusion, we was developed a selective DNA probe for the detection of PTEN gene obtained from prostate tissues using a redox copolymer [poly(glycidyl methacrylate-*co*-vinylferrocene)] as a supporting material. The DNA detection is based on monitoring the change in the current response of the modified copolymer before and after the hybridization by using CV and DPV techniques. Thus, the prepared DNA biosensor eliminates the need for an extra redox indicator used to monitor the current response in some of the DNA biosensors because the copolymer itself can directly provides a response after the hybridization. The biosensor indicated a linear range (10–100 μg mL^{-1}) with a detection limit (4.7 μg mL^{-1}) and a good selectivity toward target DNA sequence in the hybridization study carried out with target, MM, NC sequences. Also, the results of the real samples indicated that the biosensor is useful for the detection of PTEN gene in the PCR products amplified from prostate tissues. In addition, considering the compatibility of P(GMA-*co*-VFc) film as a supporting material, the proposed DNA probe can be a good example for design of new bioelectrochemical applications.

ACKNOWLEDGMENTS

The authors are grateful for the financial support by the Scientific Research Projects of Selcuk University.

REFERENCES

1. Tanaka, M.; Koul, D.; Davies, M. A.; Liebert, M.; Steck, P. A.; Grossman, H. B. *Oncogene* **2000**, *19*, 5406.
2. Dong, J. T.; Li, C. L.; Sipe, T. W.; Frierson, H. F. *Jr. Clin. Cancer Res.* **2001**, *7*, 304.
3. Backman, S. A.; Ghazarian, D.; So, K.; Sanchez, O.; Wagner, K. U.; Hennighausen, L.; Suzuki, A.; Tsao, M. S.; Chapman, W. B.; Stambolic, V.; Mak, T. W. *Proc. Natl. Acad. Sci. USA* **2004**, *101*, 1725.
4. Chen, M.; Pratt, C. P.; Zeeman, M. E.; Schultz, N.; Taylor, B. S.; O'Neill, A.; Castillo-Martin, M.; Nowak, D. G.; Naguib, A.; Grace, D. M.; Murn, J.; Navin, N.; Atwal, G. S.; Sander, C.; Gerald, W. L.; Cordon-Cardo, C.; Newton, A. C.; Carver, B. S.; Trotman, L. C. *Cancer Cell* **2011**, *20*, 173.
5. Fei, G.; Ebert, M. P.; Mawrin, C.; Leodolter, A.; Schmidt, N.; Dietzmann, K.; Malfertheiner, P. *Eur. J. Gastroenterol. Hepatol.* **2002**, *14*, 297.
6. Li, J.; Yen, C.; Liaw, D.; Podsypanina, K.; Bose, S.; Wang, S. I.; Puc, J.; Miliaresis, C.; Rodgers, L.; McCombie, R.; Bigner, S. H.; Giovanella, B. C.; Ittmann, M.; Tycko, B.; Hibshoosh, H.; Wigler, M. H.; Parsons, R. *Science* **1997**, *297*, 1943.
7. Pourmand, G.; Ziaee, A. A.; Abedi, A. R.; Mehrsai, A.; Alavi, H. A.; Ahmadi, A.; Saadati, H. R. *Urol. J.* **2007**, *4*, 95.
8. Wang, S.; Gao, J.; Lei, Q.; Rozengurt, N.; Pritchard, C.; Jiao, J.; Thomas, G.V.; Li, G.; Roy-Burman, P.; Nelson, P.S.; Liu, X.; Wu, H. *Cancer Cell* **2003**, *4*, 209.
9. Squire, J. A. *Nat. Genet.* **2009**, *41*, 509.
10. Choucair, K.; Ejdelman, J.; Brimo, F.; Aprikian, A.; Chevalier, S.; Lapointe, J. *BMC Cancer* **2012**, *12*, 543.
11. Hermanson, G. T., Ed.; Bioconjugate Techniques, 2nd ed. Academic Press: New York, CA, **2008**, Chapter 10, pp 498–505.
12. Krasnoslobodtsev, A.; Smirnov, S. *Langmuir* **2001**, *17*, 7593.

13. Zhao, X.; Tapec-Dytioco, R.; Tan, W. *J. Am. Chem. Soc.* **2003**, *125*, 11474.
14. Landers, J. P. *Anal. Chem.* **2003**, *75*, 2919.
15. Miao, W. J.; Bard, A. *J. Anal. Chem.* **2004**, *76*, 5379.
16. Wang, X.; He, P.; Fang, Y. *J. Lumin.* **2010**, *130*, 1481.
17. Su, X. D.; Robelek, R.; Wu, Y. J.; Wang, G. Y.; Knoll, W. *Anal. Chem.* **2004**, *76*, 489.
18. Chung, D. J.; Whittaker, A. K.; Choi, S. H. *J. Appl. Polym. Sci.* **2012**, *126*, E28.
19. Gong, H.; Zhong, T.; Gao, L.; Li, X.; Bi, L.; Kraatz, H. B. *Anal. Chem.* **2009**, *81*, 8639.
20. Wang, Y.; Li, C.; Li, X.; Li, Y.; Kraatz, H. B. *Anal. Chem.* **2008**, *80*, 2255.
21. Wang, L.; Liu, Q.; Hu, Z.; Zhang, Y.; Wu, C.; Yang, M.; Wang, P. *Talanta* **2009**, *78*, 647.
22. Meric, B.; Kerman, K.; Ozkan, D.; Kara, P.; Erensoy, S.; Akarca, U. S.; Mascini, M.; Ozsoz, M. *Talanta* **2002**, *56*, 837.
23. Dogan-Topal, B.; Ozkan, S. A. *Talanta* **2011**, *83*, 780.
24. Li, C.; Karadeniz, H.; Canavar, E.; Erdem, A. *Electrochim. Acta* **2012**, *82*, 137.
25. Wu, G.; Yang, N.; Zhang, T.; Wang, Z.; Lu, X.; Kang, J. *Sensor. Actuat. B* **2011**, *160*, 598.
26. Prabhakar, N.; Singh, H.; Malhotra, B. D. *Electrochem. Commun.* **2008**, *10*, 821.
27. Palecek, E.; Tomschik, M.; Stankova, V.; Havran, L. *Electroanal.* **1997**, *9*, 990.
28. Karadeniz, H.; Erdem, A.; Kuralay, F.; Jelen, F. *Talanta* **2009**, *78*, 187.
29. Takenaka, S.; Yamashita, K.; Takagi, M.; Uto, Y.; Kondo, H. *Anal. Chem.* **2000**, *72*, 1334.
30. Yau, H. C. M.; Chan, H. L.; Yang, M. *Biosens. Bioelectron.* **2003**, *18*, 873.
31. Wang, G.; Zhang, J.; Murray, R. W. *Anal. Chem.* **2002**, *74*, 4320.
32. Liu, G.; Wan, Y.; Gau, V.; Zhang, J.; Wang, L.; Song, S.; Fan, C. *J. Am. Chem. Soc.* **2008**, *130*, 6820.
33. Wang, J.; Meng, W.; Zheng, X.; Liu, S.; Li, G. *Biosens. Bioelectron.* **2009**, *24*, 1598.
34. Kuralay, F.; Erdem, A.; Abaci, S.; Özyörük, H.; Yildiz, A. *Anal. Chim. Acta* **2009**, *643*, 83.
35. Kuralay, F.; Erdem, A.; Abacı, S.; Özyörük, H.; Yildiz, A. *Electrochem. Commun.* **2009**, *11*, 1242.
36. Dursun, F.; Ozoner, S.K.; Demirci, A.; Gorur, M.; Yilmaz, F.; Erhan, E. *J. Chem. Technol. Biotechnol.* **2012**, *87*, 95.
37. Senel, M.; Abasıyanık, M. F. *Electroanal.* **2010**, *22*, 1765.
38. Cevik, E.; Senel, M.; Abasıyanık, M. F. *Curr. Appl. Phys.* **2010**, *10*, 1313.
39. Senel, M.; Cevik, E.; Abasıyanık, M. F. *Sensor. Actuat. B* **2010**, *145*, 444.
40. Kara, P.; Cavdar, S.; Meric, B.; Erensoy, S.; Ozsoz, M. *Bioelectrochemistry* **2007**, *71*, 204.
41. Vural, H. C. *Biotechnol. Biotechnol. Eq.* **2012**, *26*, 3220.
42. Fang, B.; Jiao, S.; Li, M.; Qu, Y.; Jiang, X. *Biosens. Bioelectron.* **2008**, *23*, 1175.
43. Kuralay, F.; Erdem, A.; Abacı, S.; Özyörük, H.; Yıldız, A. *J. Appl. Electrochem.* **2010**, *40*, 2039.
44. Yang, J.; Zhang, Z.; Rusling, J. F. *Electroanal.* **2002**, *14*, 1494.
45. Degefa, T. H.; Kwak, J. *J. Electroanal. Chem.* **2008**, *612*, 37.
46. Jiang, C.; Yang, T.; Jiao, K.; Gao, H. *Electrochim. Acta* **2008**, *53*, 2917.
47. Mello, M. L. S.; Vidal, B. C. *Plos. One* **2012**, *7*, 1.
48. Marco, J. P.; Borges, K. B.; Tarley, C. R. T.; Ribeiro, E. S.; Pereira, A. C. *J. Electroanal. Chem.* **2013**, *704*, 159.
49. Lyubchenko, Y.; Shlyakhtenko, L.; Harrington, R.; Oden, P.; Lindsay, S. *Proc. Natl. Acad. Sci. USA* **1993**, *90*, 2137.
50. Han, W.; Dlakic, M.; Zhu, Y. J.; Lindsay, S. M.; Harrington, R. E. *Proc. Natl. Acad. Sci. USA* **1997**, *94*, 10565.
51. Bustamante, C.; Vesenka, J.; Tang, C. L.; Rees, W.; Guthold, M.; Keller, R. *Biochemistry* **1992**, *31*, 22.
52. Bas, S. Z.; Gulce, H.; Yildiz, S. *J. Mol. Catal. B* **2011**, *72*, 282.
53. Bandyopadhyay, K.; Vijayamohanian, K. *Langmuir* **1999**, *15*, 5314.
54. Brito, R.; Tremont, R.; Cabrera, C. R. *J. Electroanal. Chem.* **2004**, *574*, 15.
55. Sanchez-Pomales, G.; Santiago-Rodriguez, L.; Rivera-Velez, N. E.; Cabrera, C. R. *J. Electroanal. Chem.* **2007**, *611*, 80.